





ORIGINAL RESEARCH

Impact of phosphate addition on PFAS treatment performance for drinking water

Levi M. Hauptert¹  | Adam Redding² | J. Margaret Gray³ | John Civardi³ | Boris Datsov⁴ | Toby T. Sanan¹  | Marc A. Mills¹ | Thomas F. Speth¹  | Jonathan B. Burkhardt¹ 

¹Office of Research and Development, Center for Environmental Solutions and Emergency Response, U.S. Environmental Protection Agency, Cincinnati, Ohio, USA

²Calgon Carbon Corporation, Drinking Water Solutions, Moon Township, Pennsylvania, USA

³Mott MacDonald, Iselin, New Jersey, USA

⁴ORAU Student Services Contractor, Oak Ridge Associated Universities, Cincinnati, Ohio, USA

Correspondence

Jonathan B. Burkhardt, Office of Research and Development, Center for Environmental Solutions and Emergency Response, U.S. Environmental Protection Agency, 26 West Martin Luther King Drive, Cincinnati, OH 45268, USA.
Email: burkhardt.jonathan@epa.gov

Deputy Editor: Lauren Weinrich

Associate Editor: Detlef R. U. Knappe

Abstract

Adding new unit operations to drinking water treatment systems requires consideration of not only efficacy for its design purpose but also costs, water quality characteristics, impact on overall regulatory compliance, and impact of other treatment unit operations. Here, pilot study results for ion exchange (IX) and granular activated carbon (GAC) are presented for a utility with both per- and polyfluoroalkyl substances (PFAS) and volatile organic contaminant removal needs. Specifically, the impact of upstream air stripping and phosphate addition on PFAS treatment performance was evaluated. Modeling was used to fit the IX and GAC pilot data and predict performance under different scenarios. GAC performance was generally consistent for treating water before or after the air stripper, but the addition of phosphate prior to air-stripping resulted in a loss of 15%–25% capacity for some PFAS on IX media, demonstrating the need to consider the entire treatment train before implementing PFAS removal unit operations.

KEYWORDS

adsorption, air stripping, anion exchange, drinking water, GAC, modeling, PFAS

1 | INTRODUCTION

Per- and polyfluoroalkyl substances (PFAS) have gained wide concern for potential health impacts. In 2022, EPA published proposed updated interim health advisory levels for PFOA and PFOS (PFAS names are defined in Table 1), and final health advisory levels for GenX chemicals and PFBS (USEPA, 2022). PFAS have been identified in numerous waters that are supplies to drinking water utilities (Cadwallader, 2022), and numerous research efforts have been conducted or are underway to identify possible treatment options (Crone et al., 2019; Vu & Wu, 2022; Wanninayake, 2021). In March 2023, EPA published a proposal for maximum contaminant levels (MCLs) of 4 ppt each for PFOA and PFOS, and a hazard

index mixture approach for PFBS, PFHxS, GenX (hexafluoropropylene oxide dimer), and PFNA (USEPA, 2023a).

Given many factors such as existing and future state regulations, proposed federal regulations, and community pressure in general, it is likely that more drinking water utilities will move to employ PFAS treatment. Granular activated carbon (GAC), anionic ion exchange resins (IX), and high-pressure membranes (reverse osmosis and nanofiltration) have been demonstrated as viable PFAS removal technologies (Appleman et al., 2014; Boyer et al., 2021; Dixit et al., 2021; Zhang et al., 2019). Of these, GAC and IX are likely to be implemented throughout the drinking water industry because many systems are familiar with implementing fixed bed GAC and IX unit operations, and high pressure membranes tend to

have higher costs and energy requirements along with a concern about disposal of membrane concentrates (Tow et al., 2021). Both GAC and IX have been shown to remove other organic contaminants, although GAC is restricted to hydrophobic/adsorbable species, and the strong-base IX resins commonly used for PFAS removal would be limited to anionic species and, to a lesser extent, zwitterionic species (Fang et al., 2021). For cases where a utility may need to remove more contaminants than just PFAS (Crone et al., 2019; McMahon et al., 2022), such as an industrially impacted surface water or a contaminated groundwater, and where more than one unit operation would be needed, optimizing the entire treatment train is necessary. Optimization can consider removal of co-adsorbing or other background constituents, formation of byproducts in upstream unit operations such as degradation products from biological or destructive technology (e.g., advanced oxidation) treatment, or addition of chemicals like poly- and/or orthophosphates.

Air stripping (AS) is a unit operation that can be used in water utilities that need to remove weakly adsorbing

Article Impact Statement

Phosphates added to an air stripper reduced PFAS removal capacity in a downstream anion exchanger in a pilot system. Pilot results can inform design decisions for PFAS removal operations.

and non-ionic volatile organic compounds (VOCs). AS has a long history in treating water to support the removal of VOCs, ammonia, or taste and odor chemicals in drinking water applications (Crittenden et al., 2012; Huang & Shang, 2006). Given that VOCs were largely regulated in the United States in the 1980's and early 1990's, many water utilities impacted by these regulations employed treatment decades ago. AS was often used in these cases. Owners of some systems with air strippers may find they also have to address PFAS and will wish to understand whether AS will benefit PFAS treatability

TABLE 1 Average water quality parameters and constituent concentrations in feeds for the IX systems.

Parameter	Pre-AS	Post-AS	Unit	Pre-AS (meq/L)	Post-AS (meq/L)
pH	6.91	7.69	–	N/A	N/A
TOC	0.994	0.904	mg/L	N/A	N/A
Chloride	203.	200.	mg/L	5.72	5.65
Sulfate	21.7	21.2	mg/L	0.45	0.44
Bicarbonate (as C) ^a	34.1	34.1	mg/L	2.84	2.84
Nitrate (as N)	4.10	3.63	mg/L	0.29	0.26
Orthophosphate	NA	0.268	mg/L	N/A	N/A
Cis-1,2 dichloroethene	0.113	<0.10	µg/L	N/A	N/A
Trichloroethene	<0.10	<0.10	µg/L	N/A	N/A
Tetrachloroethene	2.4	<0.10	µg/L	N/A	N/A
1,2 dichloroethane	<0.10	<0.10	µg/L	N/A	N/A
Perfluorobutanoic acid (PFBA)	6.76	6.67	ng/L	3.16E-08	3.12E-08
Perfluoropentanoic acid (PFPeA)	24.2	23.8	ng/L	9.17E-08	9.01E-08
Perfluorohexanoic acid (PFHxA)	13.9	13.3	ng/L	4.42E-08	4.23E-08
Perfluoroheptanoic acid (PFHpA)	6.33	6.28	ng/L	1.74E-08	1.72E-08
Perfluorooctanoic acid (PFOA)	23.6	24.2	ng/L	5.71E-08	5.85E-08
Perfluorobutanesulfonic acid (PFBS)	8.25	8.72	ng/L	2.75E-08	2.91E-08
Perfluoropentanesulfonic acid (PFPeS)	2.31	1.56	ng/L	6.60E-09	4.47E-09
Perfluoroheptanesulfonic acid (PFHpS)	1.68	1.27	ng/L	3.73E-09	2.83E-09
Perfluorononanoic acid (PFNA)	2.11	2.22	ng/L	4.54E-09	4.79E-09
Perfluorodecanoic acid (PFDA)	1.01	0.355	ng/L	1.96E-09	6.90E-10
Perfluorohexanesulfonic acid (PFHxS)	13.5	12.4	ng/L	3.37E-08	3.11E-08
Perfluorooctanesulfonic acid (PFOS)	46.1	45.2	ng/L	9.22E-08	9.04E-08

^aThe bicarbonate concentration is approximate and was derived by assuming all alkalinity was due to bicarbonate.

by removing some or all of co-occurring contaminants before PFAS unit operations. Polyphosphates can be added prior to AS to control for iron and manganese precipitation (preventing insoluble species) and calcium scale formation. Often, phosphates are sold as poly/ortho blends. Orthophosphates are useful to prevent corrosion issues, commonly used to prevent lead and copper releases. The optimal dose of both poly- and orthophosphates is a function of water quality, system materials, and intended use. Therefore, for situations where there is existing VOC treatment (USEPA, 1987, 1991a, 1991b) and PFAS treatment is being planned, the treatment train needs to be evaluated to determine the optimal approach. This includes the impact on PFAS removal as well as VOC removal and the utility's desire to keep certain unit processes for other benefits such as pH control.

To demonstrate such an approach, this work presents the results of a pilot study for a system that utilizes AS for removal of VOCs. A poly/ortho phosphate blend was added ahead of the air stripper for control of calcium scales. Four pilot units were operated to assess the impact of phosphate on the removal of PFAS through IX treatment, and the impact of the VOCs on the removal of PFAS through GAC treatment. As part of this effort, modeling was used to assess treatment performance. This work specifically highlights IX model parameter adjustments to account for both the impact of natural organic matter (NOM) and phosphate on column performance.

2 | METHODS AND MATERIALS

2.1 | Pilot system

The pilot and full-scale systems in this study were located on-site at a drinking water utility in New Jersey (NJ), USA. The water treatment plant is fed by several groundwater wells with a mixture of VOC and PFAS contaminants. Two pairs of pilot columns, one each of GAC and IX for each water type, were supplied from pre-air stripping (pre-AS) and post-air stripping (post-AS) feeds (see Figure 1). A mixed poly/ortho phosphate blend (ESC Environmental Inc., ESC 532—15%–40% sodium polyphosphate and 10%–30% phosphoric acid, monosodium salt) was added to the water prior to the AS unit with a target concentration of 0.2–0.4 mg/L as total PO_4 . Flow rates and pressures were monitored daily. Separate GAC and IX columns (Figure 1) were used for pre-AS and post-AS feeds to investigate the effect of VOCs and phosphate on GAC and IX PFAS removal efficacy.

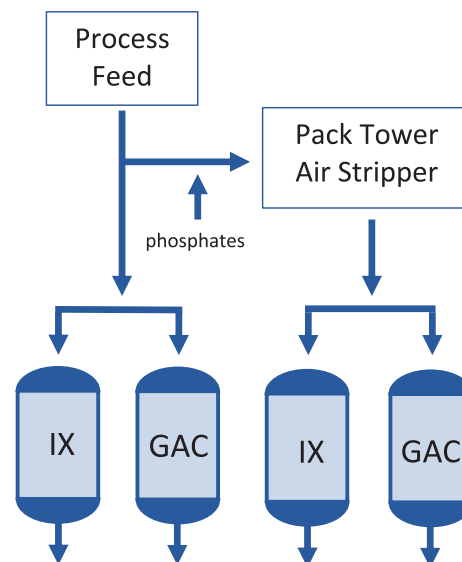


FIGURE 1 Pilot adsorption process schematic.

2.2 | GAC columns

The pilot GAC columns contained Calgon Carbon Filtrasorb 400–01 (F400–01)—a bituminous coal media at 12×40 mesh. They were 4-in. (10.2 cm) diameter columns with 36 in. (91.4 cm) of carbon (9 lb, 4.07 kg) and were operated to achieve a 3.4 min empty bed contact time (EBCT) [0.58 gpm (2.2 L/min) target]. The pre-AS column was measured to have had an average flow rate of 0.568 gpm (2.15 L/min, 3.45 min EBCT) and the post-AS column had an average flow rate of 0.547 gpm (2.07 L/min, 3.58 min EBCT) for the pre-breakthrough period (i.e., first 3–4 months) of pilot operation.

2.3 | IX columns

The pilot IX resin columns contained Calgon Carbon CalRes™ 2304 media—a gel-type strong-base anion exchange resin built on a polystyrene backbone in a chloride form. The IX columns were 4 in. (10.2 cm) diameter, 32.5 in. (82.5 cm) deep, and were operated at approximately 0.78 gpm (2.95 L/min). The pre-AS IX system had a slightly lower average flow rate over the course of the experiment than the post-AS IX system. To simplify mapping between operational time and throughput for modeling purposes, effective superficial flow velocities for the systems were determined based on flow data collected during the experiment. The effective superficial flow velocities were set to 0.588 cm/s (EBCT = 2.34 min) for the pre-AS IX train and 0.631 cm/s (EBCT = 2.18 min) for the post-AS IX train. Average particle diameter for IX resins is approximately 0.74 mm.

2.4 | Pilot system sampling

The pre-AS and post-AS feeds were sampled monthly and analyzed for chloride, sulfate, and nitrate using EPA method 300.0 R2.1; total alkalinity using standard method 2320B; and total organic carbon (TOC), an indicator of NOM, using method 5310C. The average concentrations for the major anions can be found in Table 1. Total alkalinity averaged 142 mg/L as calcium carbonate in both pre-AS and post-AS trains. For purposes of ion exchange modeling, the total alkalinity was used to obtain an approximate bicarbonate concentration in the feed waters by simply assuming that all alkalinity was due to the bicarbonate system and that nearly all the inorganic carbon was present as bicarbonate. TOC ranged from 0.6 to 1.0 mg/L with a mean 0.88 mg/L. There were no clear trends in the major anions, total alkalinity, or TOC data over the course of the pilot testing (Figure S1). One chloride ion measurement was rejected from the post-AS dataset because it was an outlier (it was 10 standard deviations away from the mean). The pH of the feed waters was measured weekly (averages: pre-AS = 6.9, post-AS = 7.7). Water temperature was also measured weekly and averaged 14.4°C for both trains. VOCs in the feeds were measured using EPA method 524.2. Chloroform, cis-1,2-dichloroethene, tetrachloroethene, and trichloroethene were detected at concentrations on the order of 1 µg/L (Table 1). The PFAS samples were collected by the utility and shipped to a contract laboratory for PFAS quantitation using EPA method 537.1. PFOS had the highest average concentration of detected PFAS at about 47 ng/L. PFOA was also present at about 24 ng/L (Table 1). Because of the importance of capturing early breakthrough dynamics and obtaining low-bias estimates of influent concentration, all analytical data above the daily analytical detection limits were used. Non-detects for PFAS that had other detections were imputed as [Detection Limit]/√2 when estimating the averages in (Table 1).

2.5 | GAC modeling

The Pore and Surface Diffusion Model (PSDM) within EPA's Water Treatment Model (USEPA, 2023b) was used to model breakthrough in GAC. A similar approach to Burkhardt et al. (2022) was used to produce effective capacity parameters (Freundlich K and $1/n$). The adsorbed mass was calculated by integrating between the pre-complete-breakthrough period influent and effluent data points for each compound—done automatically within the tool—and assuming linear interpolation between sampled values. These values were used to

establish the capacity term, q , in the Freundlich isotherm (Equation 1).

$$q = K \cdot C^{1/n}. \quad (1)$$

The chemical type was selected as PFAS, and water type was set to "Karlsruhe" to approximate the impact of NOM for a ground water with TOC of 0.7 mg/L which is similar to the TOC in the pilot system feeds. To account for the impact of fouling, the Freundlich K value was adjusted to account for the impact of TOC/NOM during the pre-breakthrough period. The breakthrough period—number of days prior to complete breakthrough—was estimated by using the calculated q , carbon mass and average mass loading associated with the average concentration in and flow rates. This resulted in Freundlich K being adjusted by approximately 1.2 to 1.55 times the initially estimated value for all compounds (consult Data S1 Section S2 for more details). A linearized isotherm assumption ($1/n = 1$) was used with these adjusted Freundlich K s and produced acceptable agreement with data, so no additional Freundlich isotherm fitting was conducted.

2.6 | IX modeling

A complete specification of the ion exchange column model (referred to here as HSDMIX) can be found in Smith et al. (2023). The model is implemented as an open-source code library and is freely available on GitHub (USEPA, 2023b). However, it is worthwhile to review some of principles of the model and ion exchange in general.

Neglecting chemical activity adjustments, the ion exchange isotherm between a hypothetical ion (B) and another ion (A) can be approximated by the apparent equilibrium coefficient (Helfferich, 1995; Zagorodni, 2006), given in terms of liquid-phase concentration (C), resin-phase concentration (q) and valence (Z) (Equation 2). The selectivity values (Equation 2) of major counterions against chloride were previously determined to be 0.033 for sulfate, 0.31 for bicarbonate, and 13 for nitrate (Smith et al., 2023).

$$K_{B,A} = \left(\frac{q_B}{C_B} \right)^{Z_A} \left(\frac{C_A}{q_A} \right)^{Z_B}. \quad (2)$$

The chromatographic separation factor between the two ions ($\alpha_{B,A}$), which has an intuitive relationship to elution order and spacing between breakthrough curves, is defined by Equation 3.

$$\alpha_{B,A} = \frac{q_B}{C_B} \frac{C_A}{q_A}. \quad (3)$$

In an ideal ion exchange column (one with no chromatographic effects or sorption front dispersion), the number of bed volumes that can be treated (Γ) for a given contaminant (i) can be expressed in terms of the bed porosity (ϵ), the influent concentration, and the equilibrium resin-phase concentration. The porosity (ϵ) of the packed bed was assumed to be 0.37 (Smith et al., 2023). Note that in this work Γ is dimensionless, and q is defined as the contaminant concentration inside the resin beads (meq/L). (Equation 4) (SenGupta, 2017). For real systems, Γ roughly corresponds to the number of bed volumes that can be treated before the column effluent rises to 50% of the average influent concentration (BV50).

$$BV50 \approx \Gamma_i = \epsilon + \frac{q_i}{C_i}(1 - \epsilon). \quad (4)$$

For a system of monovalent ions, the equilibrium q_i in the exhausted resin can be estimated from separation factors against a reference ion (A), influent concentrations, and the concentration of fixed sites in the resin (q_T) according to the multi-component isotherm given by Equation 5. The denominator in Equation 5 is a summed over all exchangeable species (indexed as j).

$$q_i = \frac{\alpha_{i,A} q_T C_i}{\sum_j \alpha_{j,A} C_j}. \quad (5)$$

Substituting Equation 5 into Equation 4 yields Equation 6.

$$\Gamma_i = \epsilon + \frac{\alpha_{i,A} q_T}{\sum_j \alpha_{j,A} C_j} (1 - \epsilon). \quad (6)$$

Recasting Equation 6 in terms of filter capacity [$Q_f = q_T(1 - \epsilon)$] and neglecting the first porosity (ϵ) term (which is negligible for sorption scenarios with more than about 100 BV to breakthrough) yields Equation 7. Q_f for the resin used in this study was previously determined to be 0.74 meq/mL of packed column (Smith et al., 2023).

$$\Gamma_i = \frac{\alpha_{i,A} Q_f}{\sum_j \alpha_{j,A} C_j}. \quad (7)$$

Sulfate, being a divalent ion, complicates analysis using Equation 7 somewhat because its chloride separation factor changes with feed composition. Approximate chloride separation factors for sulfate were obtained from Equation 3 using resin phase concentrations computed by HSDMIX during the post-breakthrough period of the major inorganic ions. The approximate values were 3.17 for the pre-AS feed, and 3.31 for the post-AS feed.

Using literature estimates for PFAS separation factors (some examples in Table 2) and the concentrations in this pilot, it is evident that the PFAS contributions to the denominator of Equation 7 are small enough to be negligible. For example, the product of the concentration of PFOA in the post-AS feed (5.85×10^{-8} meq/L) and the selectivity vs chloride from Table 2 (1.1×10^4) is only about 6.4×10^{-4} meq/L, which is far smaller than the equivalent term for chloride (5.65 meq/L). Even without considering the remaining major anions such as sulfate and NOM, the contribution of PFOA to the denominator in Equation 7 is clearly negligible. Thus, the j index in Equation 7 need only cover the major ions to obtain a reasonable estimate of Γ_i for PFAS in this system. It is important to note that, as long as this condition is true, the wave velocity of the PFAS breakthrough curve is independent of PFAS concentration (SenGupta, 2017). Equation 7 is useful because it allows for back-of-the-envelope

TABLE 2 Comparison of apparent PFAS/chloride separation factors ($\alpha_{i,A}^*$) estimated by HSDMIX and logistic function analysis for pre-AS and post-AS IX treatment trains.

PFAS	HSDMIX	HSDMIX	Logistic	Logistic	Wahman et al.	Fang et al.
	Pre-AS	Post-AS	Pre-AS	Post-AS		
PFBA	37.5 [†]	34.5 [†]	117.2	125.7	110	363
PFPeA	380.8	321.7	381.8	322.5	370*	513
PFHxA	1050.8	855.8	982.3	848.5	1500	1778
PFHpA	2272.3	1980.2	2130.9	1961.0	4500*	3311
PFOA	4913.1	3516.3	4644.1	3488.7	11,000	14,791

Note: Literature values from Wahman et al. (2023) and Fang et al. (2021), measured in organic-free water, are provided for reference. Values listed with (*) indicate estimation based on empirical correlation (Wahman et al., 2023). Values listed with (†) denote suspected optimization failures.

calculations of time to 50% breakthrough for system design and for predicting the approximate effects of changing concentrations of major anions on treatment efficacy.

In the pilot system used in this work, the terms in the denominator of Equation 7 are not known completely. The concentrations and chloride separation factors of phosphates, polyphosphates, and organic matter fractions are unknown. One potential approach to this problem would be to split the denominator of Equation 7 into known (β , containing terms for chloride, sulfate, nitrate, and bicarbonate) and unknown contributions (β^*), resulting in Equation 8.

$$\Gamma_i = \frac{\alpha_{i,A} Q_f}{\beta + \beta^*} \quad (8)$$

However, adding β^* to HSDMIX directly was found to be challenging to implement and of uncertain practical value. It was determined that optimizing an effective chloride separation factor ($\alpha_{i,A}^*$) for the PFAS was more convenient (Equation 9).

$$\Gamma_i = \frac{\alpha_{i,A}^* Q_f}{\beta} \quad (9)$$

In this framework, $\alpha_{i,A}^*/\alpha_{i,A}$ can be interpreted as an approximate performance ratio between the pilot system and an otherwise equivalent system with feed water free of phosphates and organics.

One seemingly straightforward method of estimating BV50 (and Γ) from breakthrough data would be to use simple linear interpolation on the breakthrough curves. However, this technique is not robust against variability or errors in measured PFAS concentrations. An alternative method of estimating BV50 is to fit an empirical curve-shape (e.g., a logistic function) to the data. Logistic models such as the Yoon-Nelson, Bohart-Adams, and (simplified) Thomas models are commonly used in the adsorption literature (Chu, 2020), including for adsorption of PFAS on ion-exchangers (Croll et al., 2023; Ellis et al., 2022). Further discussion on the application of such models to ion exchange removal of PFAS can be found in Data S1 (Section S3). Briefly put, even carefully parameterized logistic models have limited ability to predict important features of PFAS treatment performance by IX. For instance, the parameters controlling the width of breakthrough curves were found to be inconsistent across systems with multiple sample ports (multiple EBCTs) (Croll et al., 2023; Ellis et al., 2022). Despite these limitations, an empirical logistic form (Equation 10) was used to obtain initial estimates of BV50 (and, thus, $\alpha_{i,A}^*$ for PFAS) for further analysis with HSDMIX.

$$C(t) = \frac{\bar{C}_0}{1 + \exp(k[EBCT](BV50 - BV))} \quad (10)$$

In Equation 10, k is an empirical fit parameter and \bar{C}_0 is the average influent concentration for each PFAS. The factor of EBCT appears in Equation 10 for convenience in transforming between operational time and throughput. \bar{C}_0 was calculated from measured influent data, but included as a viable fit parameter, and k and BV50 were fit using *scipy*'s *curve_fit* function (Jones et al., 2014) using the “trf” (Trust Region Reflective) method (Branch et al., 1999) to allow for the use of bounds. Values for k and BV50 were bounded to be greater than zero. The resulting fit parameters are shown in Table 3 with estimated BV50 values. These BV50 values were then plugged in for Γ in Equation 9 to obtain initial estimates of PFAS $\alpha_{i,A}^*$ values (Table 4). Parameter estimates from HSDMIX were obtained by unweighted least squares optimization using the differential evolution algorithm (Storn & Price, 1997) as implemented in *scipy.optimize* (Jones et al., 2014). A film transfer coefficient for use with HSDMIX was estimated using the simplified Gnielinski correlation according to the procedure found in Roberts et al. (1985). The correlation of Hayduk and Laudie (1974) was used to estimate aqueous diffusion coefficients needed for the Gnielinski correlation. Additional details on the use of HSDMIX to estimate the PFAS $\alpha_{i,A}^*$ values from the pilot data are described in Section S4 of Data S1.

3 | PILOT SYSTEM RESULTS

3.1 | GAC

Figure 2 shows the results of the pilot phase testing and associated modeling. Negligible differences were observed in the pre-breakthrough period between the pre-AS and post-AS pilot GAC columns. PFPeS for

TABLE 3 Fit parameters and BV50 estimates for analysis of PFAS breakthrough curves using Equation 10.

PFAS	Pre-AS		Post-AS	
	k (h^{-1})	BV50 ($\times 1000$)	k (h^{-1})	BV50 ($\times 1000$)
PFBA	2.40E-2	7.68	1.25E-2	8.24
PFPeA	8.11E-3	25.0	6.78E-3	21.1
PFHxA	4.11E-3	64.4	3.55E-3	55.6
PFHpA	2.80E-3	139.6	2.59E-3	128.5
PFOA	9.04E-4	304.3	9.79E-4	228.6

the post-AS column has some earlier non-zero values but these are very close to the limit of quantification, and no similar impact of PFBS or other compounds was observed to suggest that AS was the direct cause of these data points. The linearized ($1/n = 1$) model with K_s developed from predicted q_s (Table SI-2) and expected impact of fouling generally fit the data well. It was not feasible to rigorously estimate uncertainties in the parameter determinations using the PSDM (or HSDMIX). Oscillations inherent in the numerical solutions of the model precluded estimation of uncertainties by gradient methods and computational cost precluded the use of residual bootstrapping. Thus, the analysis here is limited to point estimates and visual inspection. PFBA had non-zero

effluent values at the first sample period, which was likely due to the short contact time in these pilot columns. PFNA and PFHxS models fit early breakthrough well but predict a more rapid breakthrough than data suggests. PFPeS was predicted to breakthrough slightly earlier than the pre-AS data would suggest. However, the proximity to its limit of quantification makes further analysis challenging. Errors in estimating q from data or the associated breakthrough period would be expected to impact model agreement, but these would not be expected to dramatically change the conclusions of this modeling effort. The remainder of models of compounds visually agree with the data. The breakthrough data for available VOCs is shown in Data S1 Section S6.

TABLE 4 Ratio of observed effective PFAS/chloride separation factors for the pre-AS to those of the post-AS IX train.

PFAS	Ratio
PFBA	1.07
PFPeA	0.84
PFHxA	0.81
PFHpA	0.87
PFOA	0.72

Note: Logistic analysis was used for PFBA while HSDMIX analysis was used for remaining PFAS.

3.2 | IX

Although it is clear from simple inspection of Figure 3 that the pre-AS IX train demonstrated more efficient performance than the post-AS IX train, further insight can be obtained by examining the system performances through the lens of ion exchange theory and modeling. Comparisons of the optimized empirical logistic model and the ion exchange column model fit are shown in Figures 4 and 5. Best fit values for PFAS $\alpha_{i,A}^*$ obtained by optimization of the ion exchange model are compared to

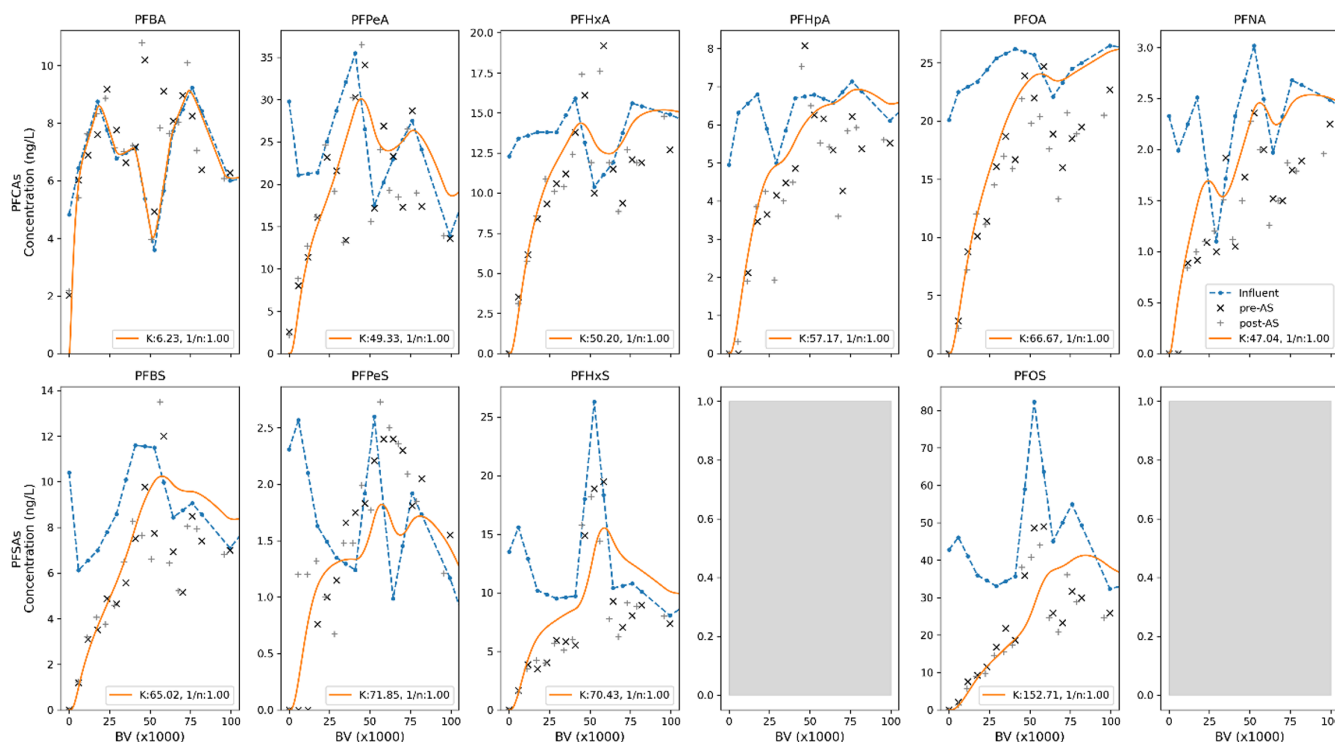


FIGURE 2 GAC comparison, pre-air stripper (pre-AS “x”), post-air stripper (post-AS “+”), and PSDM results (solid line) on a throughput basis (BV). Grayed-out fields indicate that analytical data was not available for sulfonic acid analogues of PFHpA and PFNA.

$\alpha_{i,A}^*$ estimated from optimization of the logistic function and $\alpha_{i,A}$ values taken from the literature (Fang et al., 2021; Wahman et al., 2023) Table 2. Except for PFBA, the $\alpha_{i,A}^*$ estimates obtained by HSDMIX optimization, and the logistic analysis were within 7% of each other which does support the assumptions and simplifications leading to Equation 9. The $\alpha_{i,A}^*$ estimates for the five PFAS are all on the same order of magnitude and in

the same relative order as the $\alpha_{i,A}$ obtained from batch experiments in the literature, lending further support to the applicability of standard ion exchange theory to this system.

The lack of experimental data points on the initial part of the PFBA breakthrough curve led to considerable difficulty in optimizing $\alpha_{i,A}^*$ values for PFBA with HSDMIX. The optimization consistently returned $\alpha_{i,A}^*$ on the lower bound of the search space even when this parameter was adjusted. It appears the HSDMIX was optimizing on variability in the later part of the data (which is some combination of variable influent concentration and analytical noise). Therefore, PFBA $\alpha_{i,A}^*$ listed for HSDMIX in Table 2 and the corresponding PFBA traces in Figures 4 and 5 are considered unreliable and are provided for illustrative purposes only. PFBA $\alpha_{i,A}^*$ estimates obtained using HSDMIX with fixed influent concentrations yielded results comparable to the logistic analysis (128.6 for pre-AS, 133.8 for post-AS). These difficulties highlight the importance of obtaining early breakthrough data during pilot studies.

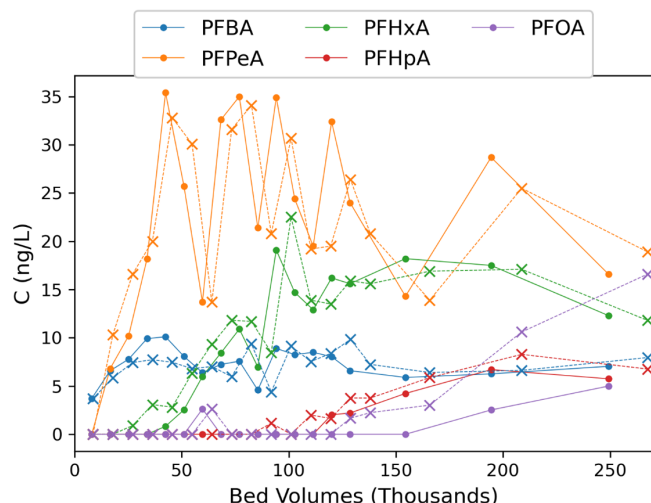


FIGURE 3 Throughput-based breakthrough curves for PFAS in the effluents of the pre-AS (“—o”) and post-AS (“---x”) IX treatment trains. PFAS not detected during the experiment are omitted.

4 | DISCUSSION

4.1 | GAC

For both the data and the modeling fits shown in Figure 2, the addition of an AS unit operation was not

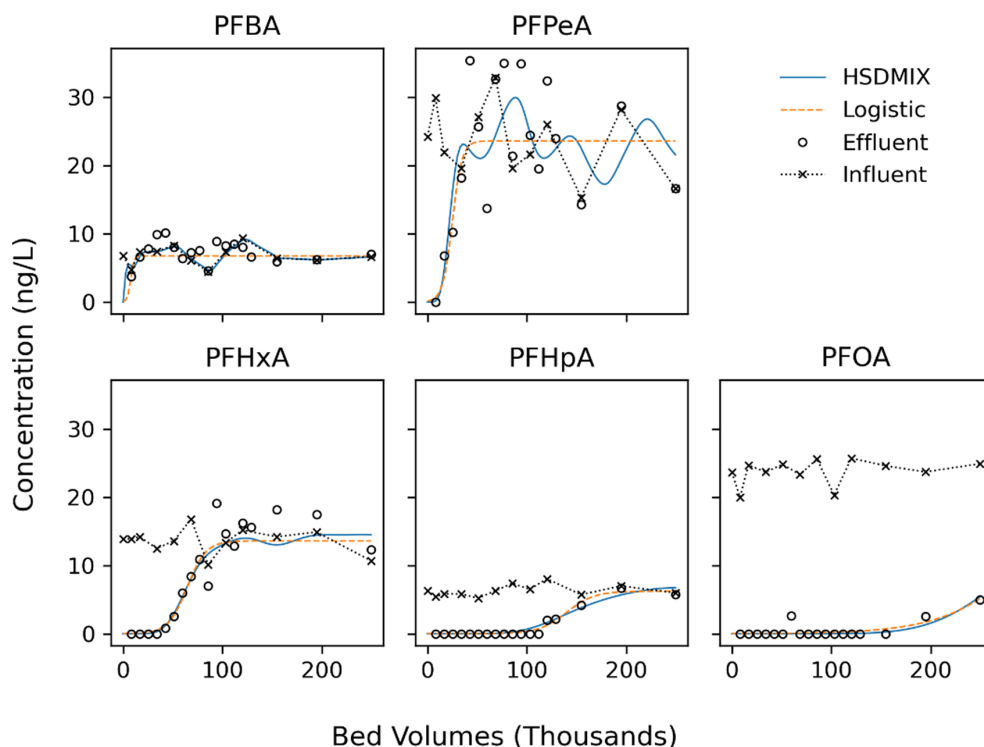
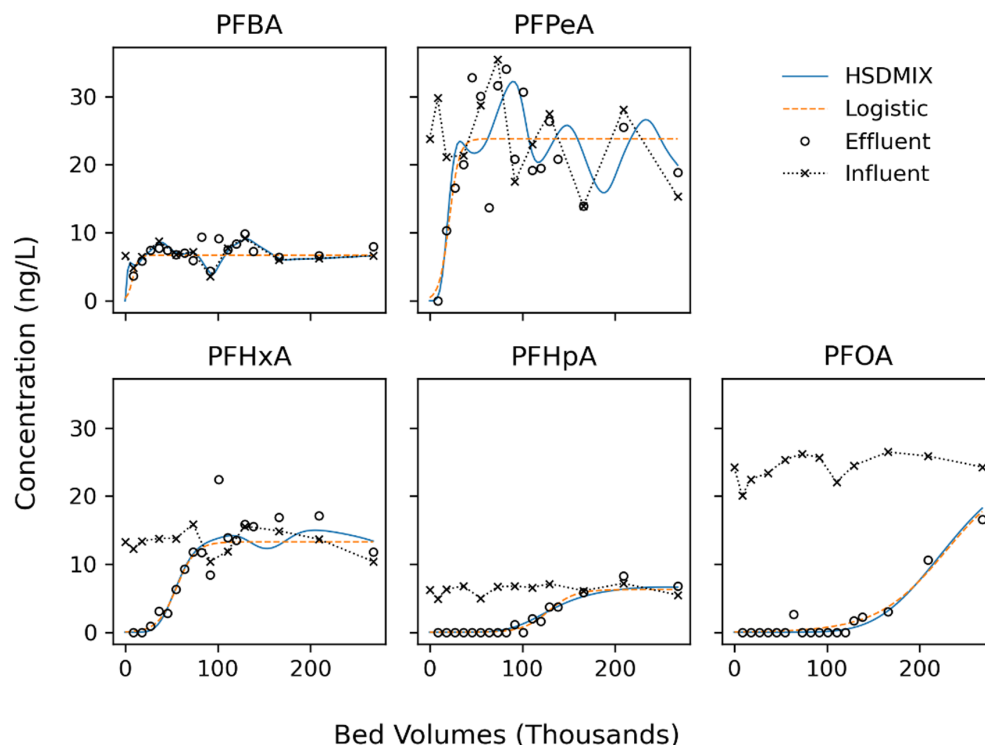


FIGURE 4 Comparison of modeled and observed breakthrough curves for PFAS in the effluents of the pre-AS IX system. PFAS system influent concentrations are included for reference.

FIGURE 5 Comparison of modeled and observed breakthrough curves for PFAS in the effluents of the post-AS IX system. PFAS system influent concentrations are included for reference.



seen to impact performance on the GAC system. Therefore, the VOCs that were present prior to AS did not seem to significantly compete with the PFAS for adsorption sites under the piloted conditions. This is consistent with Siriwardena et al. (2019), which showed limited impact of kerosene, trichloroethylene, or ethanol on PFAS adsorption onto GAC. Comparing Figures 3 and S10 highlights that all the PFAS studied here have broken through by the BV50 for tetrachloroethene (~ 100 K BV). Tetrachloroethene does not seem to be significantly reducing the capacity beyond that of the impact of NOM for this system, despite having a higher capacity on this carbon, and it may be able to access more of the carbon surface than the studied PFAS. Kazwini et al. (2022) reviewed treatment performance of various technologies with respect to PFAS removal efficacy including discussion of impacts from co-contaminants.

The post-AS water contained polyphosphates not present in the pre-AS feed (Figure 1). However, the polyphosphates did not appear to significantly compete for adsorption sites. Another difference between the two trains is pH (6.9 average for pre-AS, 7.7 average for post-AS). There was little difference in the GAC performance between the two trains, suggesting that this difference in pH did not change the ionization state of the NOM much either. These pilot systems were run at 3.4 min EBCT, which is less than the 10 min EBCTs or longer that are being considered for PFAS removal systems, but under

these conditions little difference was observed between pre-AS and post-AS GAC performance.

4.2 | IX treatment

Two key observations can be made about the IX pilot results. First, the impact of NOM on IX performance appears to be somewhat impacted to elution order and breakthrough time (both related to selectivity coefficient, $\alpha_{i,A}^*$, see Table 2). Table 5 highlights that for shorter chain compounds (PFBA and PFPeA) there is little difference in selectivity coefficients reported by Wahman et al. (2023) derived from organic free water and there was reduction in selectivity coefficients with later eluting PFCAs (PFHxA, PFHpA, and PFOA). All calculated selectivity coefficient values were lower than those reported by Fang et al. (2021). Second, the post-AS pilot experienced further reduction in selectivity coefficients (and associated capacity, see Figure 3 and Table 4) which has been attributed to the addition of phosphate during the AS unit operation. Except for PFBA, the $\alpha_{i,A}^*$ estimates for the studied PFAS, which are correlated with expected treatment efficacy, are 13%–28% lower in the post-AS ion exchange system than in the pre-AS ion exchange system (Table 4). The corresponding result for PFBA selectivity is about 7% higher based on the logistic analysis. Given the lack of breakthrough data for PFBA, and the difficulty in obtaining the $\alpha_{i,A}^*$ estimates for that compound, it

TABLE 5 Ratio of observed effective PFAS/chloride separation factors to literature values for organic-free matrices ($\alpha_{i,A}^*/\alpha_{i,A}$).

PFAS	Wahman et al.	Fang et al.
PFBA	1.12	0.34
PFPeA	1.03*	0.74
PFHxA	0.70	0.59
PFHpA	0.50*	0.69
PFOA	0.45	0.33

Note: Logistic analysis was used for PFBA while HSDMIX analysis was used for remaining PFAS. Literature values of $\alpha_{i,A}$ were taken from Wahman et al. (2023) (EPA) and Fang et al. (2021), measured in organic-free water. Values listed with (*) indicate estimation based on empirical correlation (Wahman et al., 2023). Analysis is based on pre-AS effluents.

is not clear how to interpret this difference. It is, however, clear that something in the AS process caused a deleterious effect on the IX treatment of PFPeA, PFHxA, PFHpA, and especially PFOA. The difference in VOC concentrations is unlikely to contribute to the observed effect because the VOCs were at relatively low concentrations and, being non-ionic, are not expected to compete for ion exchange sites. Furthermore, there is no plausible mechanism for how removal of VOCs at already low concentrations would reduce the effectiveness of the ion exchanger. As noted above, another difference between the two trains is pH (6.9 average for pre-AS, 7.7 average for post-AS). However, the performance of the strong base resin itself should be independent of this pH change. The PFAS studied are expected to be 100% ionized at either pH, so the adsorption affinity of the PFAS themselves should be the same. The pH difference could cause a small difference in bicarbonate concentration, but given the low resin affinity of that ion, it is very unlikely that the change could account for such large differences in PFAS removal. Accordingly, the only remaining cause of the loss of PFAS treatment efficacy on the post-AS IX system is the addition of blended phosphate. Phosphates are anions and thus can directly compete with PFAS for adsorption, making this the most likely mechanism for the capacity reduction.

The added phosphates were a blend of ortho and polyphosphates, so it is difficult to develop a precise set of modeling parameters for these interferents given the information available. It is not clear how adjusting the phosphate dose or composition would affect the performance of the IX system, and this represents an opportunity for future research in this area. For instance, would switching to 100% polyphosphate (with appropriate downstream amendments to control corrosivity) improve IX performance? This situation highlights the need for additional laboratory research on the adsorption of ortho and polyphosphates on IX resins used for PFAS removal.

Regardless, the results suggest that installing IX systems upstream of the phosphate addition would be preferable from the standpoint of media use efficiency. Additionally, available pressure and pumping must be considered, where the AS unit breaks system pressure supplied by upstream pumps and would require dedicated pumps for any downstream IX units that might be avoided or require only smaller booster pumps if the IX unit was installed upstream of the AS unit. For this system, placing the IX system upstream of the AS unit would be expected to yield higher PFAS removal performance and potentially save expenses on additional pumps and their operational and maintenance costs.

Besides the effect of the AS treatment on the efficacy of IX treatment, another interesting aspect of the results and analysis of the breakthrough data is the difference between the $\alpha_{i,A}^*$ estimates for the pre-AS IX system and the $\alpha_{i,A}$ reported for the PFAS in the literature (Table 5). PFBA is problematic here due to the wide range of literature values (110–363) and the uncertainty in the estimates of $\alpha_{i,A}^*$ obtained in this work for PFBA. Otherwise, there does appear to be a trend of increasing efficacy loss for higher affinity PFAS. The effect was quite pronounced for PFOA, which only operated at 33%–45% of the reported adsorption efficacy values. Unless there is some other unaccounted for major anion in the system, the effect is likely due to interference by NOM. Theoretically, the inhomogeneity of NOM could explain the trend of increasing interference on later-eluting PFAS. It is possible that strongly adsorbing NOM fractions could be held up near the top of the column when the earlier PFAS elute, leading to little interference to those PFAS. Unfortunately, this behavior cannot be clearly observed in the TOC breakthrough profiles (Figures S6–S9). Furthermore, there was not enough breakthrough data in the IX effluents to properly assess the effects of NOM on later-eluting PFAS, such as PFOS. More detailed bench-scale experiments on the sorption of NOM on strong base IX resins coupled with pilot studies will likely be needed before the mechanism of interference by NOM can be elucidated and a productive model developed to capture this behavior. This is an important opportunity for future work in this area as a model that also includes the impact of NOM more directly would greatly improve the ability of the community to design and interpret the results of pilot studies such as the one examined here.

5 | CONCLUSION

Adding an air stripping unit operation and removing a number of VOCs did not appear to have any observable effect on the removal of PFAS from contaminated

groundwater by GAC during this pilot. In contrast, the air stripping system including addition of phosphate reduced the treatment efficacy of the IX system for several PFAS, including PFOA, by as much as 28%. Addition of a blended phosphate (including orthophosphate) for calcium scale control is the likely cause of interference in the IX system. It was also observed that the pre-AS IX system (without phosphate) only operated at 33%–45% of its expected adsorption efficacy as estimated from literature estimates of PFAS resin affinity measured in NOM-free waters. This observed reduction in capacity for IX media related to NOM highlights the importance of considering NOM's impact on performance, where pilot studies can be used to determine achievable real-world treatment performance. Several data gaps were encountered in this work that, if addressed, would enable a more complete and more powerful evaluation. Suggestions for studies to fill these gaps are as follows: (1) controlled column experiments with NOM/TOC, (2) examination of orthophosphate/polyphosphate interactions with IX resins, and (3) investigation of PFAS diffusion in the interior of IX resin beads. Despite these needs, the modeling exercise was found to help interpret the pilot results and gain valuable insights into treatment performance.

AUTHOR CONTRIBUTIONS

Levi M. Hauptert: Data curation; formal analysis; visualization; methodology; writing – original draft; writing – review and editing. **Adam Redding:** Conceptualization; resources; methodology; writing – review and editing. **J. Margaret Gray:** Conceptualization; investigation; methodology; project administration; writing – review and editing. **John Civardi:** Data curation; investigation; methodology; writing – review and editing. **Boris Datsov:** Data curation; formal analysis; visualization; methodology; writing – review and editing. **Toby Sanan:** Data curation; validation; writing – review and editing. **Marc A. Mills:** Data curation; validation; project administration; writing – review and editing. **Thomas F. Speth:** Conceptualization; writing – original draft; project administration; writing – review and editing. **Jonathan B. Burkhardt:** Visualization; methodology; writing – original draft; writing – review and editing.

ACKNOWLEDGMENTS

The NJ utility, and the U.S. Environmental Protection Agency (EPA) through its Office of Research and Development funded the research described herein. It has been subjected to the Agency's review and has been approved for publication. Note that approval does not signify that the contents necessarily reflect the views of the Agency. Any mention of trade names, products, or services does not imply an endorsement by the U.S. Government or

EPA. The EPA does not endorse any commercial products, services, or enterprises. The contractors' role did not include establishing Agency policy. The authors gratefully acknowledge the water utility staff for their efforts in collecting the numerous water samples used in this study.

CONFLICT OF INTEREST STATEMENT

One of the authors is employed by the vendor that sells the GAC and ion exchange resins used in this study.

DATA AVAILABILITY STATEMENT

The data appearing in this publication are available on EPA's Science Hub at <https://catalog.data.gov/dataset/>.

ORCID

Levi M. Hauptert  <https://orcid.org/0000-0001-7090-7773>
 Toby T. Sanan  <https://orcid.org/0000-0002-0186-2089>
 Thomas F. Speth  <https://orcid.org/0000-0002-6640-2737>
 Jonathan B. Burkhardt  <https://orcid.org/0000-0002-2935-4422>

REFERENCES

- Appleman, T. D., Higgins, C. P., Quiñones, O., Vanderford, B. J., Kolstad, C., Zeigler-Holady, J. C., & Dickenson, E. R. (2014). Treatment of poly- and perfluoroalkyl substances in US full-scale water treatment systems. *Water Research*, 51, 246–255. <https://doi.org/10.1016/j.watres.2013.10.067>
- Boyer, T. H., Fang, Y., Ellis, A., Dietz, R., Choi, Y. J., Schaefer, C. E., Higgins, C. P., & Strathmann, T. J. (2021). Anion exchange resin removal of per- and polyfluoroalkyl substances (PFAS) from impacted water: A critical review. *Water Research*, 200, 117244. <https://doi.org/10.1016/j.watres.2021.117244>
- Branch, M. A., Coleman, T. F., & Li, Y. (1999). A subspace, interior, and conjugate gradient method for large-scale bound-constrained minimization problems. *SIAM Journal on Scientific Computing*, 21(1), 1–23. <https://doi.org/10.1137/S1064827595289108>
- Burkhardt, J. B., Burns, N., Mobley, D., Pressman, J. G., Magnuson, M. L., & Speth, T. F. (2022). Modeling PFAS removal using granular activated carbon for full-scale system design. *Journal of Environmental Engineering*, 148(3), 04021086. [https://doi.org/10.1061/\(asce\)ee.1943-7870.0001964](https://doi.org/10.1061/(asce)ee.1943-7870.0001964)
- Cadwallader, A. (2022). A Bayesian hierarchical model for estimating national PFAS drinking water occurrence. *AWWA Water Science*, 4(3), e1284. <https://doi.org/10.1002/aws2.1284>
- Chu, K. H. (2020). Breakthrough curve analysis by simplistic models of fixed bed adsorption: In defense of the century-old Bohart-Adams model. *Chemical Engineering Journal*, 380, 122513. <https://doi.org/10.1016/j.cej.2019.122513>
- Crittenden, J. C., Trussell, R. R., Hand, D. W., Howe, K. J., & Tchobanoglous, G. (2012). *Water treatment: Principles and design* (3rd ed.). John Wiley & Sons.
- Croll, H. C., Adelman, M. J., Chow, S. J., Schwab, K. J., Capelle, R., Oppenheimer, J., & Jacangelo, J. G. (2023). Fundamental kinetic constants for breakthrough of per- and Polyfluoroalkyl

- substances at varying empty bed contact times: Theoretical analysis and pilot scale demonstration. *Chemical Engineering Journal*, 464, 142587. <https://doi.org/10.1016/j.cej.2023.142587>
- Crone, B. C., Speth, T. F., Wahman, D. G., Smith, S. J., Abulikemu, G., Kleiner, E. J., & Pressman, J. G. (2019). Occurrence of per-and polyfluoroalkyl substances (PFAS) in source water and their treatment in drinking water. *Critical Reviews in Environmental Science and Technology*, 49(24), 2359–2396. <https://doi.org/10.1080/10643389.2019.1614848>
- Dixit, F., Dutta, R., Barbeau, B., Berube, P., & Mohseni, M. (2021). PFAS removal by ion exchange resins: A review. *Chemosphere*, 272, 129777. <https://doi.org/10.1016/j.chemosphere.2021.129777>
- Ellis, A. C., Liu, C. J., Fang, Y., Boyer, T. H., Schaefer, C. E., Higgins, C. P., & Strathmann, T. J. (2022). Pilot study comparison of regenerable and emerging single-use anion exchange resins for treatment of groundwater contaminated by per-and polyfluoroalkyl substances (PFASs). *Water Research*, 223, 119019. <https://doi.org/10.1016/j.watres.2022.119019>
- Fang, Y., Ellis, A., Choi, Y. J., Boyer, T. H., Higgins, C. P., Schaefer, C. E., & Strathmann, T. J. (2021). Removal of per-and polyfluoroalkyl substances (PFASs) in aqueous film-forming foam (AFFF) using ion-exchange and nonionic resins. *Environmental Science & Technology*, 55(8), 5001–5011. <https://doi.org/10.1021/acs.est.1c00769>
- Hayduk, W., & Laudie, H. (1974). Prediction of diffusion coefficients for nonelectrolytes in dilute aqueous solutions. *AIChE Journal*, 20(3), 611–615. <https://doi.org/10.1002/aic.690200329>
- Helferich, F. G. (1995). *Ion exchange*. Courier Corporation.
- Huang, J.-C., & Shang, C. (2006). Air stripping. In L. K. Wang, Y.-T. Hung, & N. K. Shamma (Eds.), *Advanced physicochemical treatment processes* (pp. 47–79). Humana Press.
- Jones, E., Oliphant, T., & Peterson, P. (2014). SciPy: Open source scientific tools for Python, 2014. <http://www.scipy.org>
- Kazwini, T., Yadav, S., Ibrar, I., Al-Juboori, R. A., Singh, L., Ganbat, N., Kazwini, T., Karbassiyazdi, E., Samal, A. K., Subbiah, S., & Altaee, A. (2022). Updated review on emerging technologies for PFAS contaminated water treatment. *Chemical Engineering Research and Design*, 182, 667–700. <https://doi.org/10.1016/j.cherd.2022.04.009>
- McMahon, P. B., Tokranov, A. K., Bexfield, L. M., Lindsey, B. D., Johnson, T. D., Lombard, M. A., & Watson, E. (2022). Perfluoroalkyl and polyfluoroalkyl substances in groundwater used as a source of drinking water in the eastern United States. *Environmental Science & Technology*, 56(4), 2279–2288. <https://doi.org/10.1021/acs.est.1c04795>
- Roberts, P. V., Cornel, P., & Summers, R. S. (1985). External mass-transfer rate in fixed-bed adsorption. *Journal of Environmental Engineering*, 111(6), 891–905. [https://doi.org/10.1061/\(ASCE\)0733-9372\(1985\)111:6\(891\)](https://doi.org/10.1061/(ASCE)0733-9372(1985)111:6(891))
- SenGupta, A. K. (2017). *Ion exchange in environmental processes: Fundamentals, applications and sustainable technology*. John Wiley & Sons.
- Siriwardena, D. P., Crimi, M., Holsen, T. M., Bellona, C., Divine, C., & Dickenson, E. (2019). Influence of groundwater conditions and co-contaminants on sorption of perfluoroalkyl compounds on granular activated carbon. *Remediation Journal*, 29(3), 5–15. <https://doi.org/10.1002/rem.21603>
- Smith, S. J., Wahman, D. G., Kleiner, E. J., Abulikemu, G., Stebel, E. K., Gray, B. N., Datsov, B., Crone, B. C., Taylor, R. D., Womack, E., Gastaldo, C. X., Sorial, G., Lytle, D., Pressman, J. G., & Hauptert, L. M. (2023). Anion exchange resin and inorganic anion parameter determination for model validation and evaluation of unintended consequences during PFAS treatment. *ACS ES&T Water*, 3, 576–587. <https://doi.org/10.1021/acsestwater.2c00572>
- Storn, R., & Price, K. (1997). Differential evolution—A simple and efficient heuristic for global optimization over continuous spaces. *Journal of Global Optimization*, 11(4), 341–359. <https://doi.org/10.1023/A:1008202821328>
- Tow, E. W., Ersan, M. S., Kum, S., Lee, T., Speth, T. F., Owen, C., Bellona, C., Nadagouda, M. N., Mikelonis, A. M., Westerhoff, P., Mysore, C., Frenkel, V. S., de Silva, V., Walker, W. S., Safulko, A. K., & Westerhoff, P. (2021). Managing and treating per-and polyfluoroalkyl substances (PFAS) in membrane concentrates. *AWWA Water Science*, 3(5), e1233. <https://doi.org/10.1002/aws2.1233>
- USEPA. (1987). Phase I: National primary drinking water regulations; synthetic organic chemicals; monitoring for unregulated contaminants (final rule). *Federal Register*, 52(130), 25690–25717.
- USEPA. (1991a). Phase II: National primary drinking water regulations-synthetic organic chemicals and inorganic chemicals; monitoring for unregulated contaminants; national primary drinking water regulations implementation; national secondary drinking water regulations (final rule). *Federal Register*, 56(20), 3526–3597.
- USEPA. (1991b). Phase IIB: Drinking water; national primary drinking water regulations; monitoring for volatile organic chemicals; MCLGs and MCLs for aldicarb, aldicarb sulfoxide, aldicarb sulfone, pentachlorophenol, and barium (final rule). *Federal Register*, 56(126), 30266–30281.
- USEPA. (2022). Drinking water health advisories for PFOA and PFOS. <https://www.epa.gov/sdwa/drinking-water-health-advisories-pfoa-and-pfos>
- USEPA. (2023a). PFAS national primary drinking water regulation rulemaking (proposed rule). *Federal Register*, 88(60), 18638–18754.
- USEPA. (2023b). Water treatment models GitHub repository. https://github.com/USEPA/Water_Treatment_Models
- Vu, C. T., & Wu, T. (2022). Recent progress in adsorptive removal of per-and poly-fluoroalkyl substances (PFAS) from water/wastewater. *Critical Reviews in Environmental Science and Technology*, 52(1), 90–129. <https://doi.org/10.1080/10643389.2020.1816125>
- Wahman, D. G., Smith, S. J., Kleiner, E. J., Abulikemu, G., Stebel, E. K., Gray, B. N., Crone, B. C., Taylor, R. D., Womack, E. A., Gastaldo, C. X., Sanan, T. T., Pressman, J. G., & Hauptert, L. M. (2023). Strong base anion exchange selectivity of nine Perfluoroalkyl chemicals relevant to drinking water. *ACS ES&T Water*. In Press.
- Wanninayake, D. M. (2021). Comparison of currently available PFAS remediation technologies in water: A review. *Journal of Environmental Management*, 283, 111977. <https://doi.org/10.1016/j.jenvman.2021.111977>
- Zagorodni, A. A. (2006). *Ion exchange materials: Properties and applications*. Elsevier.
- Zhang, D., Zhang, W., & Liang, Y. (2019). Adsorption of perfluoroalkyl and polyfluoroalkyl substances (PFASs) from aqueous

solution: A review. *Science of the Total Environment*, 694, 133606. <https://doi.org/10.1016/j.scitotenv.2019.133606>

SUPPORTING INFORMATION

Additional supporting information can be found online in the Supporting Information section at the end of this article.

How to cite this article: Hauptert, L. M., Redding, A., Gray, J. M., Civardi, J., Datsov, B., Sanan, T. T., Mills, M. A., Speth, T. F., & Burkhardt, J. B. (2023). Impact of phosphate addition on PFAS treatment performance for drinking water. *AWWA Water Science*, e1361. <https://doi.org/10.1002/aws2.1361>